

Application of screened hybrid functionals to the bulk transition metals Rh, Pd, and Pt

Fabien Tran, David Koller, and Peter Blaha

Institute of Materials Chemistry, Vienna University of Technology, Getreidemarkt 9/165-TC, A-1060 Vienna, Austria

(Received 6 August 2012; published 10 October 2012)

We present the results of calculations on bulk transition metals Rh, Pd, and Pt using the screened hybrid functional YS-PBE0 [F. Tran and P. Blaha, *Phys. Rev. B* **83**, 235118 (2011)]. The results for the equilibrium geometry are compared with those obtained from (semi)local functionals, namely, the local density approximation and the generalized gradient approximation PBE of Perdew *et al.* [J. P. Perdew, K. Burke, and M. Ernzerhof, *Phys. Rev. Lett.* **77**, 3865 (1996)]. It is shown that the screened hybrid functional yields more accurate equilibrium geometry than PBE, but, overall, it is not more accurate than the local density approximation. However, in contradiction with experiment, we find that the screened hybrid functional favors a ferromagnetic state as the ground state for all three transition metals. Therefore, the use of hybrid functionals for, e.g., the study of catalytically active systems with correlated oxides on a metal support is questionable.

DOI: 10.1103/PhysRevB.86.134406

PACS number(s): 71.15.Ap, 71.15.Mb, 71.15.Nc

I. INTRODUCTION

The Kohn-Sham (KS) version of density functional theory (DFT) is the most used quantum method for the calculations of properties of matter;^{1,2} however, since we do not know the exact exchange-correlation functional, one needs to make a choice for an approximate form for practical calculations (see Ref. 3 for a recent review). Many different types of approximate exchange-correlation functionals have been proposed. The two most commonly used approximations in solid-state physics are the local density approximation (LDA)² and generalized gradient approximation (GGA), which lead, in most cases, to reasonably accurate results for the structural parameters in particular (see, e.g., Refs. 4 and 5).

However, a well-known problem of LDA and GGA is their inability to yield accurate excited-states properties, but actually this is a more general problem which has its roots in the KS method itself when an orbital-independent potential is used (see Ref. 6). The most common way to get more accurate excited-state properties is to work in the framework of the generalized KS scheme⁷ by using functionals which lead to orbital-dependent potentials like DFT + U (Ref. 8) or the hybrids.⁹ DFT + U is computationally as cheap as a LDA/GGA but can be applied only to well-localized strongly correlated electrons (typically $3d$ or $4f$ electrons). The hybrid functionals, which mix semilocal (i.e., LDA or GGA) and Hartree-Fock (HF) exchange, can be used more widely; however, for solids, they lead to calculations which are 1 or 2 orders of magnitude more expensive than LDA/GGA and their applications to metals can be problematic.¹⁰

A way to partially reduce the problems encountered with hybrid functionals for solids is to get rid of the long-range HF interaction by screening the Coulomb potential with, e.g., an exponential¹¹ or error function.¹² Actually, screened hybrid functionals are becoming more and more popular and have shown to be successful for structural and electronic properties on a large variety of solids (see Refs. 13–20 for extensive tests), including difficult cases like transition-metal (TM) oxides and nitrides as well as rare-earth and actinide oxides, where band gaps and magnetism are strongly enlarged, in agreement with experiment (see, e.g., Refs. 21–27). In the case of a GGA-based

screened hybrid functional, the functional reads

$$E_{xc} = E_{xc}^{GGA} + \alpha_x (E_x^{SR-HF} - E_x^{SR-GGA}), \quad (1)$$

where E_x^{SR-HF} and E_x^{SR-GGA} are the short-range (SR) parts of the HF and GGA exchange functionals, respectively, and α_x ($\in [0, 1]$) is the fraction of exact exchange. The most known screened hybrid functional is the one proposed by Heyd *et al.* (HSE),¹² which is based on the GGA functional PBE of Perdew *et al.*²⁸ [like the unscreened hybrid functional PBE0 (Refs. 29 and 30)] and uses the error function for the splitting of the Coulomb potential. Most of the time, HSE is used with $\alpha_x = 0.25$. Another known screened hybrid functional is the early one proposed by Bylander and Kleinman,¹¹ which is based on the LDA functional and uses a screening parameter that is calculated from the average value of the valence electron density (in HSE the screening parameter is fixed to a “universal” value).

The trend of the HSE06³¹ functional is to be very accurate for band gaps smaller than ~ 5 eV but to underestimate larger band gaps. Actually, the larger the band gap, the more the underestimation (in percentage) becomes severe (see Refs. 18 and 32). Usually, GGA functionals underestimate the atomic magnetic moments in strongly correlated systems, while the values with HSE06 (or any other hybrid functional) are increased and hence in better agreement with experiment.²⁴ Concerning the lattice constants,^{19,20} HSE06 is more accurate than PBE, but not as accurate as the GGA functionals which were especially designed for solids like WC (Ref. 33) or PBEsol.³⁴ However, we note that the values of the lattice constants depend strongly on the GGA functional on which the hybrid functional is based, while the band gaps are rather insensitive (see Ref. 19). Actually, recent studies reported calculations on solids using hybrid functionals based either on the WC (Ref. 35) or PBEsol (Ref. 19) GGA functional, and in both cases it was shown that the hybrid functional benefits from the good performances of the underlying GGA (WC or PBEsol) for geometrical parameters. We also mention that in Ref. 36, a middle-range hybrid functional was shown to perform very well on semiconductors for the lattice constant and band gap. Recently (Ref. 37), a screened hybrid functional

based on the GGA PBE functional, but using the exponential function for the splitting of the Coulomb potential (known as the Yukawa potential), was implemented into the WIEN2K code.³⁸ The choice of using the exponential function instead of the error function was made for technical reasons (e.g., integrals calculated more easily) but is of very little importance for applications. Indeed, it was shown that using the screening parameter $\lambda = 0.165 \text{ bohr}^{-1}$ (λ was kept fixed at this value for the present work) in the Yukawa potential $e^{-\lambda|\mathbf{r}-\mathbf{r}'|}/|\mathbf{r}-\mathbf{r}'|$ leads to results which are close to the results obtained with HSE06,³¹ for which $\mu = 0.11 \text{ bohr}^{-1}$ in the SR potential $\text{erfc}(\mu|\mathbf{r}-\mathbf{r}'|)/|\mathbf{r}-\mathbf{r}'|$. The functional was called YS-PBE0 (where YS stands for Yukawa screened).

In this work, we present the results of calculations obtained with the screened hybrid functional YS-PBE0 on the fcc 4d-TM Rh and Pd and 5d-TM Pt. Usually, the semilocal functionals describe fairly well the electronic and magnetic properties of the (non)magnetic 3d, 4d, and 5d TM, although in particular for GGA functionals a tendency to overestimate magnetism can be found.^{39–43} This is in contrast to the TM oxides (in particular, the 3d like MnO, NiO,⁴⁴ or the undoped cuprates⁴⁵), where magnetism is underestimated and semilocal functionals give qualitatively wrong results due to the localized nature of the d electrons, while in the pure TM the electrons are itinerant (i.e., more free-electron-like).

II. RESULTS

The calculations were done with the WIEN2K code,³⁸ which is based on the full-potential (linearized) augmented plane-wave and local-orbitals method to solve the KS equations.⁴⁶ For comparison purposes, calculations with the semilocal functionals LDA [using PW92 (Ref. 47) for correlation] and the GGA PBE (Ref. 28) were also done. The semilocal calculations were done with a $24 \times 24 \times 24$ \mathbf{k} mesh for the integrations of the Brillouin zone, while a $12 \times 12 \times 12$ \mathbf{k} mesh was used for the hybrid functional YS-PBE0 to make the computational time reasonable. We checked that using such a \mathbf{k} mesh leads to results which are accurate enough for our purposes. The size of the basis set is determined by the product $R_{\text{MT}}^{\text{min}} K_{\text{max}}$ of the smallest of the atomic sphere radii (R_{MT}) and the plane-wave cutoff parameter (K_{max}). The values 9 (100–180 basis functions per atom) and 10 (160–280 basis functions per atom) for $R_{\text{MT}}^{\text{min}} K_{\text{max}}$ were used for the hybrid and semilocal calculations, respectively. The atomic sphere radius R_{MT} was chosen as 2.2 bohr for Rh and 2.1 bohr for Pd and Pt.

The results of the calculations obtained with the LDA, PBE, and YS-PBE0 functionals are shown in Table I and Figs. 1–3. We start the discussion about the equilibrium geometry of the experimentally observed nonmagnetic (NM) phase. The experimental values for a_0 (taken from Ref. 48) were extrapolated to $T = 0$ K (using the volume expansion coefficient) and corrected for the zero-point oscillations according to the scheme of Alchagirov *et al.*⁴⁹ For Rh, we can see that the hybrid functional YS-PBE0 gives a fairly accurate value of 3.799 Å (3.786 Å for experiment), while LDA underestimates a_0 by 0.03 Å and PBE overestimates by 0.045 Å. In the case of Pd, LDA, which leads to an underestimation of ~ 0.035 Å, is more accurate than PBE and YS-PBE0, which lead to rather large overestimations (>0.06 Å). For the 5d-TM Pt,

TABLE I. Equilibrium lattice constant a_0 (in Å), bulk modulus B_0 (in GPa), and the total-energy difference (in mRy/atom) between the minima of the FM and NM phases. The experimental values are for $T = 0$ K and are corrected for the zero-point oscillations (Ref. 48).

Method	a_0^{NM}	a_0^{FM}	B_0^{NM}	B_0^{FM}	$E_{\text{tot}}^{\text{NM}} - E_{\text{tot}}^{\text{FM}}$
Rh					
LDA	3.757		316		
PBE	3.831		257		
YS-PBE0	3.799	3.874	279	226	0.59
Expt.	3.786		277		
Pd					
LDA	3.840		228		
PBE	3.943	3.946	168	165	0.15
YS-PBE0	3.935	3.938	165	168	3.96
Expt.	3.876		187		
Pt					
LDA	3.896		305		
PBE	3.971		246		
YS-PBE0	3.948	3.959	265	261	3.51
Expt.	3.917		286		

LDA is more accurate (underestimation of only ~ 0.02 Å) than PBE and YS-PBE0, which yield too large equilibrium lattice constant. By comparing our values for a_0 to the PBE and HSE06 results from Ref. 19 for Rh and Pd, we can see that the agreement is perfect (as expected) with PBE (less than 0.001 Å of difference), while our YS-PBE0 lattice constants are about 0.015 Å larger than with HSE06. As explained in Ref. 37, the differences between the YS-PBE0 and HSE06 lattice constants are mainly due to the different schemes used to screen the semilocal exchange energy. In YS-PBE0, the simple scheme of Ikura *et al.*⁵⁰ was used, while in HSE06 the screening is done by considering the expression of the functional in terms of the exchange hole.⁵¹

At this point it is useful to recall that the trends observed above with the semilocal functionals are actually rather general among the elemental TM (see, e.g., Ref. 4). For the 3d series, PBE is the most accurate, while LDA strongly underestimates the lattice constants. For the 4d TM, GGA functionals, which are softer than PBE [e.g., WC (Ref. 33) or PBEsol (Ref. 34)], are more accurate than LDA and PBE, while for the 5d, LDA is the most accurate method. It has also been observed (see, e.g., Ref. 19) that for most solids (Li and Na are two exceptions), replacing a fraction of semilocal exchange by HF exchange leads to a reduction of the equilibrium lattice constant, which is what has also been observed in the present work with Rh, Pd, and Pt (i.e., the YS-PBE0 lattice constants are smaller than the PBE ones). Therefore, the hybrid functionals based on PBE (HSE and YS-PBE0) correct the PBE overestimation for the lattice constants.^{13,19} This also explains why the lattice constants calculated with the screened-exchange LDA (Ref. 11, 100% of LDA exchange replaced by HF exchange) are in most cases by far too small,¹⁵ since on average LDA already underestimates them. The results for the bulk modulus B_0 (see Table I) show the usual trends: an underestimation (overestimation) of B_0 is associated to an overestimation (underestimation) of a_0 .

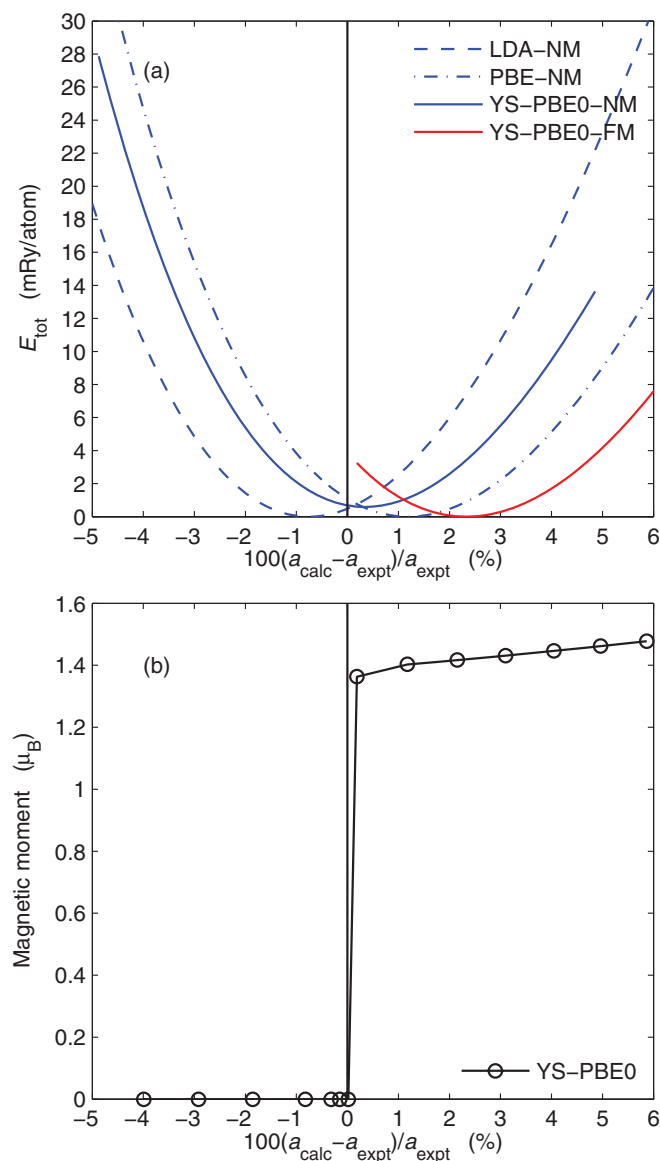


FIG. 1. (Color online) (a) Total energy and (b) magnetic moment in the unit cell of the FM and NM phases of Rh versus the lattice constant (expressed as the relative difference with respect to the experimental value) calculated from several functionals. For each functional, the zero of the energy was set to the lowest minimum. The vertical line indicates the experimental lattice constant.

Spin-polarized calculations on Rh, Pd, and Pt were also done in attempts to stabilize a ferromagnetic (FM) solution. The results, whenever available, are shown in Table I and Figs. 1–3. In the case of Rh, it was not possible to stabilize a solution with a nonzero magnetic moment with LDA for the range of lattice constants that we considered (up to 15% larger than a_{expt}), while with PBE it is for values of a larger than a_{expt} by about 13% (i.e., much larger than the equilibrium lattice constant) that such a solution could be obtained. With YS-PBE0 it was possible to stabilize a magnetic moment for lattice constants larger than the experimental one. Interestingly, the minimum of the FM total-energy curve is lower than the minimum of the NM curve by 0.59 mRy/atom [see Fig. 1(a) and Table I]. This can be considered as a

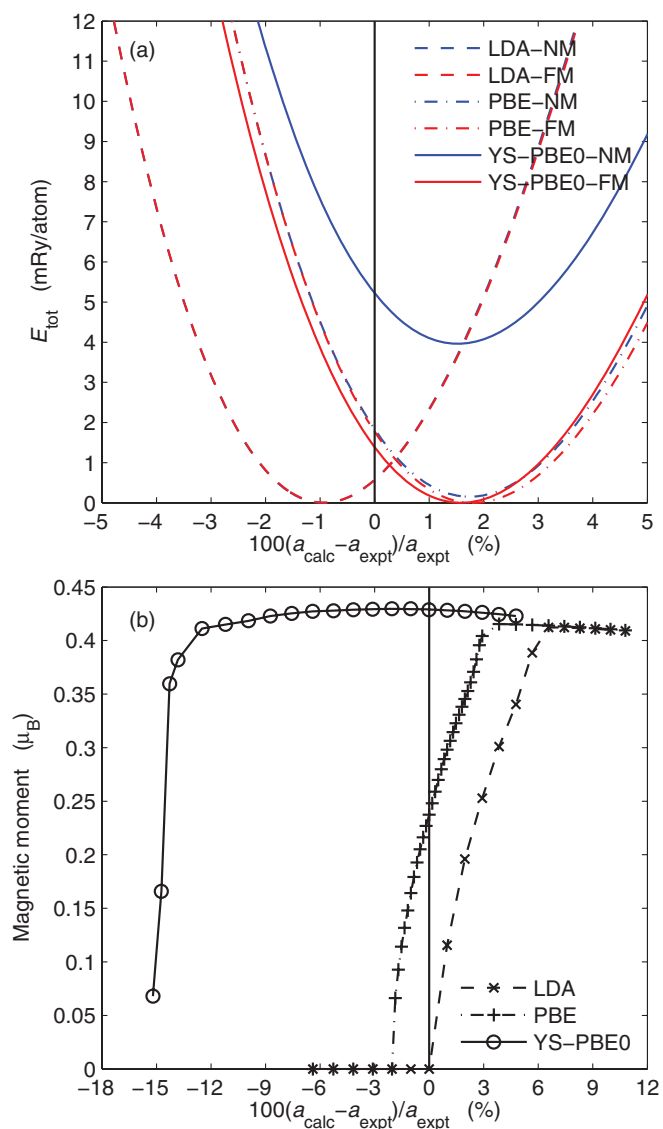


FIG. 2. (Color online) Same as Fig. 1 but for Pd. Note that in (a) and (b) the ranges for the x axis are different.

failure of the screened hybrid functional which describes Rh as magnetic, and in addition, the equilibrium lattice constant is more than 2% larger than in experiment. The value of the magnetic moment in the unit cell is around 1.4 μ_B [see Fig. 1(b)] for lattice constants larger than a_{expt} and drops suddenly to zero (NM solution) at this geometry.

Turning now to Pd, which is known experimentally and theoretically to be on the verge of becoming FM,⁵² we were able to stabilize a FM solution with all considered functionals. From Fig. 2(b), we can see that the smallest lattice constant at which it was possible to obtain a FM solution is around -15% , -1.7% , and 1% of a_{expt} for YS-PBE0, PBE, and LDA, respectively, and therefore, at both the experimental geometry as well as at the corresponding theoretical geometry, the magnetic moment is nonzero for PBE and YS-PBE0. Note that the values of the magnetic moments obtained at larger values of a with the different functionals are quite similar (0.40–0.45 μ_B). As for Rh with YS-PBE0, the FM minimum is lower than the NM minimum for PBE and YS-PBE0

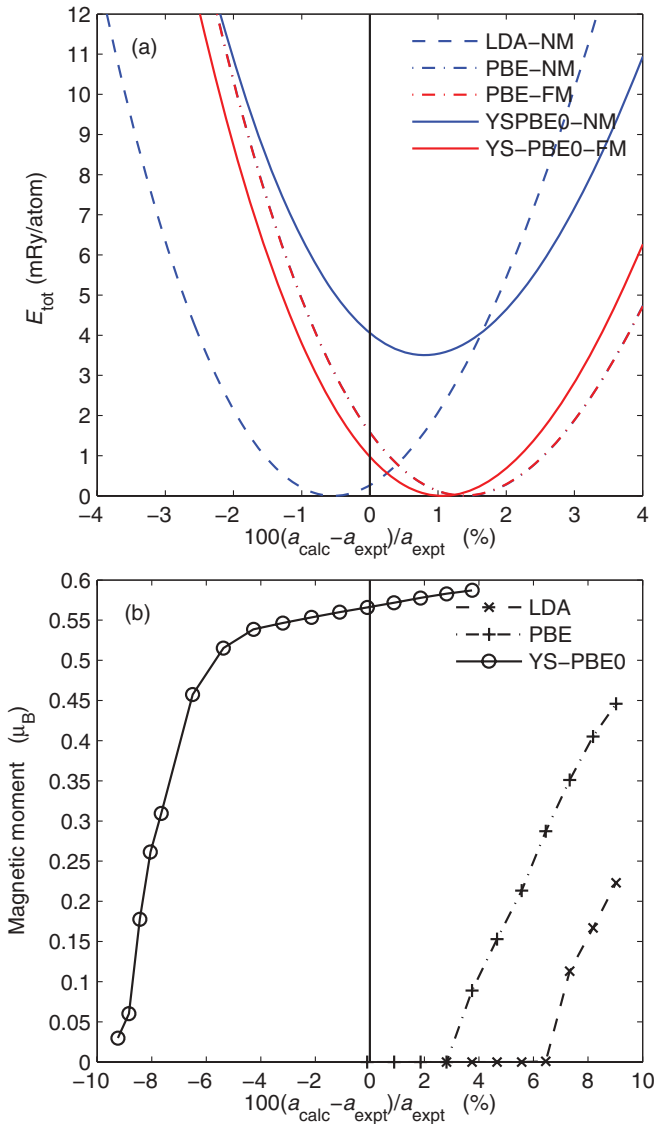


FIG. 3. (Color online) Same as Fig. 1 but for Pt. Note that in (a) and (b) the ranges for the x axis are different.

functionals by 0.15 and 3.96 mRy/atom, respectively. The latter value is 1 order of magnitude larger than in the case of Rh, and again this can be considered as a quite severe failure of the screened hybrid functional.

For Pt [see Fig. 3(b)], nonzero magnetic moments can be obtained for lattice constants larger than approximately -9% , 3% , and 7% of a_{expt} for YS-PBE0, PBE, and LDA, respectively, and thus at the experimental or theoretical lattice constant only YS-PBE0 gives a wrong magnetic ground state. Therefore,

from Fig. 3(a) we can see again that with YS-PBE0 the FM state is more stable than the NM state and their minima differ substantially by 3.51 mRy/atom.

III. SUMMARY

From the results presented above, we can conclude that the screened hybrid functional YS-PBE0 slightly improves over PBE for the equilibrium lattice constants of solids, which were too large with PBE (a rather general trend with PBE). But note that for the $4d$ -TM Pd and $5d$ -TM Pt, LDA is more accurate than PBE and YS-PBE0. However, the main result of the present work is the inability of YS-PBE0 to give the correct ground state for the three considered TM. Indeed, the FM state is found to be lower in energy than the experimentally observed NM state. It is well known (see Ref. 10 and references therein) that the use of the HF approximation for metals leads to severe problems, such as a vanishing density of states at the Fermi level or too large magnetic moments. (A remedy would be to use a compatible correlation functional like the random-phase approximation,⁵³ but such methods are very expensive and their self-consistent implementation not trivial at all.)

These problems are due, in particular, to the long-range part of the HF exchange, which is not present in screened hybrid functionals. However, it was shown¹⁴ that the screened hybrid functionals still lead to an overestimation of the exchange splitting (and the corresponding magnetic moment) in itinerant magnetic systems such as Fe for which semilocal methods work quite well.

While the use of the gradient correction was necessary to correctly obtain the bcc FM phase as the ground state in Fe (Refs. 54 and 55, the ground state is fcc NM with LDA), our work has shown more evidence that using screened exact exchange as an additional ingredient in functionals is not recommended for itinerant metals. This has important implications for the studies of correlated TM oxides on TM surfaces, which is relevant for many important catalytic active surfaces, where oxides on metals such as Rh, Pd, or Pt play a crucial role. While the hybrid functionals describe in such systems the correlated oxides pretty well, the results suffer from the overestimation of magnetism for the underlying metals.⁵⁶ Thus the DFT + U methods, where the strength of the correlation effects unfortunately has to be selected by hand for each atom, seem to be the only practical way at the moment to describe such systems.

ACKNOWLEDGMENT

This work was supported by the project SFB-F41 (ViCoM) of the Austrian Science Fund.

¹P. Hohenberg and W. Kohn, *Phys. Rev.* **136**, B864 (1964).

²W. Kohn and L. J. Sham, *Phys. Rev.* **140**, A1133 (1965).

³A. J. Cohen, P. Mori-Sánchez, and W. Yang, *Chem. Rev.* **112**, 289 (2012).

⁴P. Haas, F. Tran, and P. Blaha, *Phys. Rev. B* **79**, 085104 (2009); **79**, 209902(E) (2009).

⁵G. I. Csonka, J. P. Perdew, A. Ruzsinszky, P. H. T. Philipsen, S. Lebègue, J. Paier, O. A. Vydrov, and J. G. Ángyán, *Phys. Rev. B* **79**, 155107 (2009).

⁶S. Kümmel and L. Kronik, *Rev. Mod. Phys.* **80**, 3 (2008).

⁷A. Seidl, A. Görling, P. Vogl, J. A. Majewski, and M. Levy, *Phys. Rev. B* **53**, 3764 (1996).

- ⁸V. I. Anisimov, J. Zaanen, and O. K. Andersen, *Phys. Rev. B* **44**, 943 (1991).
- ⁹A. D. Becke, *J. Chem. Phys.* **98**, 1372 (1993).
- ¹⁰I. C. Gerber, J. G. Ángyán, M. Marsman, and G. Kresse, *J. Chem. Phys.* **127**, 054101 (2007).
- ¹¹D. M. Bylander and L. Kleinman, *Phys. Rev. B* **41**, 7868 (1990).
- ¹²J. Heyd, G. E. Scuseria, and M. Ernzerhof, *J. Chem. Phys.* **118**, 8207 (2003); **124**, 219906 (2006).
- ¹³J. Heyd, J. E. Peralta, G. E. Scuseria, and R. L. Martin, *J. Chem. Phys.* **123**, 174101 (2005).
- ¹⁴J. Paier, M. Marsman, K. Hummer, G. Kresse, I. C. Gerber, and J. G. Ángyán, *J. Chem. Phys.* **124**, 154709 (2006); **125**, 249901 (2006).
- ¹⁵S. J. Clark and J. Robertson, *Phys. Rev. B* **82**, 085208 (2010).
- ¹⁶S. J. Clark and J. Robertson, *Phys. Status Solidi B* **248**, 537 (2011).
- ¹⁷T. M. Henderson, J. Paier, and G. E. Scuseria, *Phys. Status Solidi B* **248**, 767 (2011).
- ¹⁸M. A. L. Marques, J. Vidal, M. J. T. Oliveira, L. Reining, and S. Botti, *Phys. Rev. B* **83**, 035119 (2011).
- ¹⁹L. Schimka, J. Harl, and G. Kresse, *J. Chem. Phys.* **134**, 024116 (2011).
- ²⁰R. Peverati and D. G. Truhlar, *J. Chem. Phys.* **136**, 134704 (2012).
- ²¹K. N. Kudin, G. E. Scuseria, and R. L. Martin, *Phys. Rev. Lett.* **89**, 266402 (2002).
- ²²I. D. Prodan, G. E. Scuseria, J. A. Sordo, K. N. Kudin, and R. L. Martin, *J. Chem. Phys.* **123**, 014703 (2005).
- ²³I. D. Prodan, G. E. Scuseria, and R. L. Martin, *Phys. Rev. B* **73**, 045104 (2006).
- ²⁴M. Marsman, J. Paier, A. Stroppa, and G. Kresse, *J. Phys.: Condens. Matter* **20**, 064201 (2008).
- ²⁵V. Eyert, *Phys. Rev. Lett.* **107**, 016401 (2011).
- ²⁶M. Schlipf, M. Betzinger, C. Friedrich, M. Ležaić, and S. Blügel, *Phys. Rev. B* **84**, 125142 (2011).
- ²⁷A. S. Botana, F. Tran, V. Pardo, D. Baldomir, and P. Blaha, *Phys. Rev. B* **85**, 235118 (2012).
- ²⁸J. P. Perdew, K. Burke, and M. Ernzerhof, *Phys. Rev. Lett.* **77**, 3865 (1996); **78**, 1396 (1997).
- ²⁹M. Ernzerhof and G. E. Scuseria, *J. Chem. Phys.* **110**, 5029 (1999).
- ³⁰C. Adamo and V. Barone, *J. Chem. Phys.* **110**, 6158 (1999).
- ³¹A. V. Krukau, O. A. Vydrov, A. F. Izmaylov, and G. E. Scuseria, *J. Chem. Phys.* **125**, 224106 (2006).
- ³²E. N. Brothers, A. F. Izmaylov, J. O. Normand, V. Barone, and G. E. Scuseria, *J. Chem. Phys.* **129**, 011102 (2008).
- ³³Z. Wu and R. E. Cohen, *Phys. Rev. B* **73**, 235116 (2006); Y. Zhao and D. G. Truhlar, *ibid.* **78**, 197101 (2008); Z. Wu and R. E. Cohen, *ibid.* **78**, 197102 (2008).
- ³⁴J. P. Perdew, A. Ruzsinszky, G. I. Csonka, O. A. Vydrov, G. E. Scuseria, L. A. Constantin, X. Zhou, and K. Burke, *Phys. Rev. Lett.* **100**, 136406 (2008); **102**, 039902(E) (2009); A. E. Mattsson, R. Armiento, and T. R. Mattsson, *ibid.* **101**, 239701 (2008); J. P. Perdew, A. Ruzsinszky, G. I. Csonka, O. A. Vydrov, G. E. Scuseria, L. A. Constantin, X. Zhou, and K. Burke, *ibid.* **101**, 239702 (2008).
- ³⁵D. I. Bilc, R. Orlando, R. Shaltaf, G.-M. Rignanese, J. Íñiguez, and P. Ghosez, *Phys. Rev. B* **77**, 165107 (2008).
- ³⁶M. J. Lucero, T. M. Henderson, and G. E. Scuseria, *J. Phys.: Condens. Matter* **24**, 145504 (2012).
- ³⁷F. Tran and P. Blaha, *Phys. Rev. B* **83**, 235118 (2011).
- ³⁸P. Blaha, K. Schwarz, G. K. H. Madsen, D. Kvasnicka, and J. Luitz, *WIEN2K: An Augmented Plane Wave Plus Local Orbitals Program for Calculating Crystal Properties*, edited by K. Schwarz (Vienna University of Technology, Austria, 2001).
- ³⁹D. J. Singh and J. Ashkenazi, *Phys. Rev. B* **46**, 11570 (1992).
- ⁴⁰I. I. Mazin and D. J. Singh, *Phys. Rev. B* **69**, 020402(R) (2004).
- ⁴¹A. Aguayo, I. I. Mazin, and D. J. Singh, *Phys. Rev. Lett.* **92**, 147201 (2004).
- ⁴²A. Subedi and D. J. Singh, *Phys. Rev. B* **81**, 024422 (2010); **81**, 059902(E) (2010).
- ⁴³L. Ortenzi, I. I. Mazin, P. Blaha, and L. Boeri, *Phys. Rev. B* **86**, 064437 (2012).
- ⁴⁴K. Terakura, T. Oguchi, A. R. Williams, and J. Kübler, *Phys. Rev. B* **30**, 4734 (1984).
- ⁴⁵W. E. Pickett, *Rev. Mod. Phys.* **61**, 433 (1989); **61**, 749 (1989).
- ⁴⁶D. J. Singh and L. Nordström, *Planewaves, Pseudopotentials and the LAPW Method*, 2nd ed. (Springer, Berlin, 2006).
- ⁴⁷J. P. Perdew and Y. Wang, *Phys. Rev. B* **45**, 13244 (1992).
- ⁴⁸K. Lejaeghere, V. Van Speybroeck, G. Van Oost, and S. Cottenier, arXiv:1204.2733.
- ⁴⁹A. B. Alchagirov, J. P. Perdew, J. C. Boettger, R. C. Albers, and C. Fiolhais, *Phys. Rev. B* **63**, 224115 (2001).
- ⁵⁰H. Iikura, T. Tsuneda, T. Yanai, and K. Hirao, *J. Chem. Phys.* **115**, 3540 (2001).
- ⁵¹M. Ernzerhof and J. P. Perdew, *J. Chem. Phys.* **109**, 3313 (1998).
- ⁵²A. Oswald, R. Zeller, and P. H. Dederichs, *Phys. Rev. Lett.* **56**, 1419 (1986).
- ⁵³T. Kotani and H. Akai, *J. Magn. Magn. Mater.* **177–181**, 569 (1998).
- ⁵⁴P. Bagno, O. Jepsen, and O. Gunnarsson, *Phys. Rev. B* **40**, 1997 (1989).
- ⁵⁵B. Barbiellini, E. G. Moroni, and T. Jarlborg, *J. Phys.: Condens. Matter* **2**, 7597 (1990).
- ⁵⁶C. Franchini, J. Zabloudil, R. Podloucky, F. Allegretti, F. Li, S. Surnev, and F. P. Netzer, *J. Chem. Phys.* **130**, 124707 (2009).